

Cosmological Perturbation Theory and the Spherical Collapse model- II. Non-Gaussian initial conditions.

Enrique Gaztañaga and Pablo Fosalba

*Institut d'Estudis Espacials de Catalunya, Research Unit (CSIC),
Edf. Nexus-201 - c/ Gran Capità 2-4, 08034 Barcelona, Spain*

13 June 2021

ABSTRACT

In Part I of this series, we introduced the Spherical Collapse (SC) approximation in Lagrangian space as a way of estimating the cumulants ξ_J of density fluctuations in cosmological Perturbation Theory (PT). Within this approximation, the dynamics is decoupled from the statistics of the initial conditions, so we are able to present here the cumulants for generic Non-Gaussian initial conditions, which can be estimated to arbitrary order including the smoothing effects. The SC model turns out to recover the exact leading-order non-linear contributions up to terms involving non-local integrals of the J -point functions. We argue that for the hierarchical ratios S_J , these non-local terms are sub-dominant and tend to compensate each other. The resulting predictions show a non-trivial time evolution that can be used to discriminate between models of structure formation. We compare these analytic results to Non-Gaussian N-body simulations, which turn out to be in very good agreement up to scales where $\sigma \lesssim 1$.

Key words: cosmology:large-scale structure of Universe-cosmology: theory-galaxies: clustering-methods:analytical-methods: numerical.

1 INTRODUCTION

The large scale galaxy distribution can be used to study the origin and dynamics of cosmological fluctuations. The one-point statistical clustering of matter density fluctuations δ_R , smoothed over scale R , is characterized here in terms of the reduced J th-order moments $\bar{\xi}_J(R) \equiv \langle \delta_R^J \rangle_c$. Assuming that gravity is the dominant dynamical effect, the evolution of $\bar{\xi}_J(R, t)$ is completely fixed by the initial conditions (IC): $\bar{\xi}_J(0, R)$. The problem is that even in the simplest case of pressureless (collisionless) matter, we do not have the exact solution to the dynamical equations. Here we concentrate on the approximation given by perturbation theory (PT) which provides a framework to study small departures from the linear theory solution. The question we want to address is: what are the predictions of PT for a given set of (Non-Gaussian) IC? This is important because large scale galaxy surveys can then be used to discriminate between models of structure formation (*e.g.*, Silk & Juszkiewicz 1991).

We already have a good idea of how to answer this question for Gaussian initial conditions (GIC), both at leading order, or tree-level (Peebles 1980, Fry 1984, Bernardeau 1992), and also with higher-order (loop) corrections (Scoccamarro & Frieman 1996a, 1996b, Fosalba & Gaztañaga 1998). Comparison with observations and simulations made it necessary to develop PT also for the smoothed fields (*e.g.*, Go-

roff *et al.* 1986, Juszkiewicz *et al.* 1993, Bernardeau 1994a, 1994b).

The analytic calculations in the literature for Non-Gaussian initial conditions (NGIC) refer to the variance, ξ_2 , skewness S_3 , (see Fry & Scherrer 1994, FS94 hereafter) and the kurtosis, S_4 , (see Chodorowsky & Bouchet 1996, CB96 hereafter). These studies are important from the theoretical point of view, but of little help in practice because they only apply to the *unsmoothed* fields. Numerical work by Weinberg & Cole (1992) provided interesting insights on different aspects of some particular Non-Gaussian models but did not address the general question of the initial conditions (other works include Moscardini *et al.* 1993). Gaztañaga and Mähönen (1996), studied the case of strongly NGIC in N-body simulations as compared to GIC, showing important differences that could be used to discriminate models with current observations.

Here we follow the path set up in Paper I (Fosalba & Gaztañaga 1998) and study the case of a generic Non-Gaussian model for the IC, under the spherical collapse (SC) approximation, which will allow us to present predictions for the smoothed fields. In §2 we set the problem of NGIC and recall the SC model. In §3 we present the predictions for a generic case of NGIC and compare them to N-body simulations and some previous calculations. We end up with a discussion and the final conclusions in §4.

2 NON-GAUSSIAN INITIAL CONDITIONS

For a given clustering in the initial conditions, we would like to derive the final clustering using the exact dynamics that rule the evolution of the underlying field. To characterize the clustering, we concentrate on the study the statistical properties of one-point J th-order moments $m_J \equiv \langle \delta^J \rangle$ of smoothed density fluctuations δ . In particular we will use a combination of moments, the so call *connected moments* or *reduced cumulants* $\bar{\xi}_J$, which of a given J carry statistical information independent of the lower order moments, and are formally denoted by a bracket with subscript c . These cumulants can be easily obtained by using the generating function method:

$$\bar{\xi}_J = \langle \delta^J \rangle_c = \left. \frac{d^J}{dt^J} \ln \langle e^{t\delta} \rangle \right|_{t=0}. \quad (1)$$

A *dimensional scaling* of the higher-order moments in terms of the second order one $\bar{\xi}_2 = \sigma^2$ is given by the following ratios:

$$B_J \equiv \frac{\bar{\xi}_J}{\sigma^J} = \frac{\bar{\xi}_J}{\bar{\xi}_2^{J/2}}. \quad (2)$$

For Gaussian initial conditions (GIC) in PT, it is more useful to introduce the *hierarchical coefficients*,

$$S_J = \frac{\bar{\xi}_J}{\bar{\xi}_2^{J-1}} = B_J [\bar{\xi}_2]^{1-J/2} \quad (3)$$

as PT predicts them to be time-independent quantities on large scales, for GIC. These amplitudes are also called normalized one-point cumulants or reduced cumulants. We shall also use *skewness*, for S_3 and *kurtosis*, for S_4 .

As in Paper I, we start by expanding the density contrast δ assuming that it is small, as is usually done in the context of perturbation theory (PT) in Euler space,

$$\delta(\mathbf{x}, t) = \delta_1(\mathbf{x}, t) + \delta_2(\mathbf{x}, t) + \delta_3(\mathbf{x}, t) \dots, \quad (4)$$

where we consider $\delta_n \ll \delta_{n-1}$. The first term $\delta_1 \equiv \delta_l$ is the solution to the linearized field equations. The second term $\delta_2 \sim \delta_l^2$ is the second-order solution, obtained by using the linear solution in the source terms, and so on.

In Fourier space, we write, $\delta(\mathbf{k}) \equiv \sum_{n=1}^{\infty} \delta_n(\mathbf{k})$, being $\delta_n(\mathbf{k})$ the n -th order perturbative contribution. The latter is expressed as an n -dimensional integral over the kernels, F_n , that encode the nonlinear coupling of modes due to the gravitational evolution,

$$\begin{aligned} \delta_n(\mathbf{k}) &= \int d^3q_1 \dots d^3q_n \delta_D(\mathbf{k} - \mathbf{q}_1 \dots - \mathbf{q}_n) \times \\ &\times F_n(\mathbf{q}_1 \dots \mathbf{q}_n) \delta_1(\mathbf{q}_1) \dots \delta_1(\mathbf{q}_n) \end{aligned} \quad (5)$$

where δ_D is the Dirac function and the kernels F_n are given by symmetric homogeneous functions of \mathbf{q}_n with degree zero, that is, some geometrical average (see Fry 1984, Goroff *et al.* 1986, Jain & Bertschinger 1994, Scoccimarro & Frieman 1996a).

2.1 Linear Theory

If we only consider the first term in the PT series, Eq.[4], and the growing mode, the cumulants of the evolved field will just be:

$$\bar{\xi}_J \equiv \langle \delta^J \rangle_c = \langle \delta_l^J \rangle_c = D^J \langle \delta_0^J \rangle_c, \quad (6)$$

where D is the linear growth factor and $\langle \delta_0^J \rangle_c$ correspond to the cumulants of the IC. Consistently, the hierarchical ratios (see Eq.[3]) will scale as:

$$S_J = S_J(0)/D^{J-2}, \quad (7)$$

where $S_J(0)$ are the initial ratios. Note that this implies that the linear growth erases the initial hierarchical ratios, so that $S_J \rightarrow 0$, as time evolves (and $D \rightarrow \infty$).

In terms of the dimensional scaling, see Eq.[2], we have, $B_J = B_J(0)$, so that the linear growth preserves the initial values. Note that if we want to do a meaningful calculation of these ratios or the cumulants, in general, we might need to consider more terms in the perturbation series, Eq.[4], depending on the statistical properties of the IC, *e.g.*, how they scale with the initial variance, which is typically the smallness parameter in the expansion of the cumulants.

For GIC both $B_J(0) = S_J(0) = 0$, and we have to consider higher-order terms in the perturbation series to be able to make a non-vanishing prediction.

2.2 Gaussian Tree-Level

The computation of the cumulants in PT dates back to Peebles (1980) work where the leading order contribution to the skewness was obtained making use of the second-order PT, *e.g.*, F_2 . Fry 1984 extended Peebles analysis by making the connection between tree diagrams (or tree-graphs) and the perturbative contributions to leading order in the GIC case. With the help of this formalism he was able to obtain the leading order contributions for the three- and four-point functions making use of the 2nd and 3rd order kernels, F_2 and F_3 , in PT. Furthermore, Fry found that, in general, the lowest order (tree-level) connected part that contributes to ξ_J are of order $2(J-1)$ in δ_1 . Note that this involves the cancellation of $J-2$ contribution to the moment of order J , m_J . This is a property of the GIC for which all $\langle \delta_1^J \rangle_c$ vanish for $J > 2$. For GIC the leading order contribution is only given by tree-graphs and is therefore called the 'tree-level' (see also Paper I).

Bernardeau (1992) found the generating function of the one-point cumulants to leading order for GIC. Here (and in Paper I) we present a simpler derivation, inspired in Bernardeau's work, that can be extended to higher-order (loop) corrections and NGIC.

2.3 The Monopole Approximation & The Spherical Collapse Model

Given the kernels F_n in Eq.[5], we define the *monopole* contribution to F_n as the spherically symmetric (angle) average:

$$F_n^{l=0} \equiv \langle F_n \rangle = c_n/n!. \quad (8)$$

The monopole approximation, δ is the one resulting by substituting F_n by $\langle F_n \rangle$. Under this approximation, we obviously have, from Eq.[5]:

$$\delta_n(\mathbf{k}) = \frac{c_n}{n!} \delta_l(\mathbf{k}) * \dots * \delta_l(\mathbf{k}), \quad (9)$$

where $*$ means convolution (in Fourier space), so that, in real space $\delta(\mathbf{k}) \equiv \sum_{n=1}^{\infty} \delta_n(\mathbf{k})$ becomes:

$$\delta(\mathbf{x}) \equiv \sum_{n=1}^{\infty} \delta_n(\mathbf{x}) = f[\delta_1(\mathbf{x})] = \sum_{n=1}^{\infty} \frac{c_n}{n!} [\delta_1(\mathbf{x})]^n. \quad (10)$$

Thus, the monopole contribution to the cumulants in PT is given by a local-density transformation Eq.[10], whose coefficients c_n are to be determined by the kernels F_n , which are found by solving the perturbative equations under the relevant dynamics (in Fourier space).

We can now easily estimate *all* the 1-point statistical properties in the *monopole* approximation to PT. This can be done by using the generating function method Eq.[1], with the field δ given by Eq.[10]. When the initial conditions are hierarchical, the resulting expressions can be found in Fry & Gaztañaga (1993), who consider a generic local-density transformation and find, to leading terms in σ_l :

$$\begin{aligned} S_3 &= S_3^{IC} + 3c_2 + \mathcal{O}(\sigma_l^2) \\ S_4 &= S_4^{IC} + 12c_2 S_3^{IC} + 4c_3 + 12c_2^2 + \mathcal{O}(\sigma_l^2) \\ S_5 &= S_5^{IC} + 20c_2 S_4^{IC} + 15c_2 S_3^{IC2} + (30c_3 + 120c_2^2) S_3^{IC} \\ &\quad + 5c_4 + 60c_3 c_2 + 60c_2^3 + \mathcal{O}(\sigma_l^2) \end{aligned} \quad (11)$$

where S_J^{IC} are the hierarchical amplitudes in linear theory (which are given by the IC). If the IC are not hierarchical one might have to consider more terms to estimate the leading order (see §3). These arguments are valid for any dynamics and also for both Euler or Lagrangian space, they apply to any leading order calculation where Eq.[5] is valid.

To estimate the PT contribution to the cumulants (*e.g.*, c_n) it is not necessary to calculate the structure of the kernels F_n from the exact solution to the field equations of δ , as in Goroff *et al.* (1986). Given the equations for the evolution of the field one can determine Eq.[10] and therefore c_n by just requiring the solutions to be *spherically symmetric*. In Paper I, it was shown that for gravity, the spherically symmetric solution to the dynamical equations is given by the Spherical Collapse (SC), whose solution is well-known [*e.g.*, see §4.1 in Paper I]. Thus, $c_n = \nu_n$, without need of estimating the kernels F_n or any integral. In particular, the ν_n coefficients are derived by Taylor-expanding the parametric solution to the SC model around $\delta_l = 0$ (see Paper I, §4.1). The connection between the Gaussian tree-level in PT and the SC model was already pointed out by Bernardeau (1992, 1994a, 1994b) although, there, the tree-level amplitudes were derived using the rather complicated formalism of the *vertex generating function* instead of the density contrast itself.

For GIC we also showed in Paper I how the *monopole* approximation gives the exact leading order, which is given by the tree-level solution. We next will argue that it also gives the exact contribution to the tree-graphs that appear for NGIC.

2.4 Cumulants for a Non-Gaussian Tree-Level

On estimating the PT predictions for cumulants $\bar{\xi}_J$, Fry (1984) described the connection between tree diagrams (or tree-graphs) and the perturbative contributions to leading order in the Gaussian case. These Gaussian *tree-level* terms will also contribute to the estimation $\bar{\xi}_J$ in the case of NGIC, as they come from the products of linear terms, δ_1 , induced by the two-point function. But there are additional terms in the Non-Gaussian case. For example, consider the kurtosis:

$$\langle \delta^4 \rangle = \langle (\delta_1 + \delta_2 + \dots)^4 \rangle = \langle \delta_1^4 \rangle + 4 \langle \delta_1^3 \delta_2 \rangle + \dots \quad (12)$$

Now, δ_2 is given by the 2nd order kernel F_2 in Eq.[5]: $\delta_2 \sim F_2 \delta_1^2$ so that the term $\langle \delta_1^3 \delta_2 \rangle$ above involves an integral over $F_2 \langle \delta_1^5 \rangle$, which is zero in the Gaussian case, but gives in general:

$$\langle \delta_1^5 \rangle = \langle \delta_1^5 \rangle_c + 10 \langle \delta_1^3 \rangle_c \langle \delta_1^2 \rangle_c. \quad (13)$$

Consider first the second term of the above equation. The only connected part of the above term that contributes to the $F_2 \langle \delta_1^5 \rangle$ integral in the kurtosis, is just given by a tree-graph, connected with no loops, of the type:

$$\int d^3 q_1 d^3 q_2 \delta_D(\mathbf{k}_1 - \mathbf{q}_1 - \mathbf{q}_2) F_2(\mathbf{q}_1, \mathbf{q}_2) \langle \delta_1(\mathbf{q}_1) \delta_1(\mathbf{k}_2) \delta_1(\mathbf{k}_3) \rangle \langle \delta_1(\mathbf{q}_2) \delta_1(\mathbf{k}_4) \rangle, \quad (14)$$

here again, like in the Gaussian case [Eq.[23] in Paper I], the last two factors do not have any dependence on the angle, $\mathbf{q}_1 \mathbf{q}_2$, and the contribution of the kernel F_2 is just given by the geometric average, *e.g.*, the number $c_2/2$. This illustrates that *the local transformation, Eq.[10], given by the monopole, also accounts for the exact contribution from the tree-graphs in the Non-Gaussian case, e.g.*, the contribution $12c_2 S_3^{IC}$ to S_4 in the local expression (11). It also accounts for the direct terms from linear theory [first terms to the right hand of equations (11)], which are zero in the Gaussian case, and are not regarded as tree-graphs.

Nevertheless, for Non-Gaussian IC the tree-graphs do not necessarily include all the leading-order contributions, unlike the Gaussian case. There are terms like $\langle \delta_1^5 \rangle_c$ in Eq.[13], which also comes from $\langle \delta_1^3 \delta_2 \rangle$ and contribute to the kurtosis Eq.[12]. The contribution involves an integral of $F_2 \langle \delta_1^5 \rangle_c$. In the monopole approximation, Eq.[10], this term is simply given by $c_2/2 \langle \delta_1^5 \rangle_c$. While in the exact calculation, its value could have contributions from higher multipoles, depending on the particular form of the initial conditions $\langle \delta_1^5 \rangle_c$, which is needed to do the integration. FS94 have estimated this multipole integration for several Non-Gaussian models for the initial kurtosis, $\xi_4^l = \langle \delta_1^4 \rangle_c$. They typically find (see their Table 1) that the coefficients $I[\xi_4^l]/\xi_4^l$, which corresponds to the relative contribution of the higher multipoles, are smaller than unity, thus typically smaller than the monopole contribution $c_n/n! \gtrsim 1$ (see below Eq.[33]). This is not surprising as correlations typically decrease with distance, thus reducing the contribution from non-spherical geometries. Thus, in general, one expects the monopole to be the dominant contribution. In the case of hierarchical initial conditions, $\langle \delta_1^5 \rangle_c$ is of order σ_l^8 , while $\langle \delta_1^3 \rangle_c \langle \delta_1^2 \rangle_c$ is of order σ_l^6 . Thus in this case the monopole (local) approximation *exactly* accounts for all the leading-order terms.

2.5 Smoothing Effects

In §4.4 of Paper I, it was shown how to relate the *smoothed* cumulants of the evolved distribution with the *smoothed* cumulants in the initial one. The arguments presented there were general and could be applied to both Gaussian and Non-Gaussian initial conditions. In the case of a power-law power spectrum $P(k) \sim k^n$, the smoothed variance is also a power-law $\hat{\sigma}_l \sim R^{\gamma/2}$, where $\gamma = -(n+3)$. We then have:

$$\delta[\hat{\delta}_i] \sim f[\hat{\delta}_i(1 + \delta)^{\gamma/6}] \quad (15)$$

up to a normalization factor given by Eq.[39] in Paper I. Note that this final result as well as the general expression agrees with Bernardeau (1994a) arguments, based on the vertex generating function, but they do not limit us to Gaussian initial conditions or the leading-order term. Here again, the vertex generating function $\mathcal{G}(-\tau)$, corresponds to cumulants in Euler space, while our local-density relation $f(\delta_i)$, applies to Lagrangian space. To leading order, they both give identical results for Gaussian IC, but they yield different results in general for Non-Gaussian IC or for higher-order terms with Gaussian IC.

3 PREDICTIONS FOR NON-GAUSSIAN INITIAL CONDITIONS

Here we study the more general case of evolution in PT from Non-Gaussian initial conditions (NGIC), where $\bar{\xi}_J(0) \neq 0$. If we use $\delta_n \sim \delta_1^n$, the first perturbative contributions are:

$$\begin{aligned} \bar{\xi}_J(t) &\simeq D^J \bar{\xi}_J(0) + J/2 d_2 D^{J+1} \bar{\xi}_{J+1}(0) + \dots \\ &+ D^{2(J-1)} S_J^G \bar{\xi}_2^{J-1}(0) + \dots \end{aligned} \quad (16)$$

where $S_J^G \equiv S_{J,0}^G$ (see notation in §3.1) are the Gaussian tree-level amplitudes,

$$\begin{aligned} S_3^G &= \frac{34}{7} + \gamma \\ S_4^G &= \frac{60712}{1323} + \frac{62}{3} \gamma + \frac{7}{3} \gamma^2 \end{aligned} \quad (17)$$

and so on, for a power-law power spectrum and a top-hat window (see also *e.g.*, §5 in Paper I.) These amplitudes are intrinsically gravitational as the GIC ones are zero for $J > 2$.

In the case of NGIC, it is more difficult to present a perturbation series because it depends on how $\bar{\xi}_J(0)$ scales with $\bar{\xi}_2(0)$. In a statistically homogeneous distribution, $\bar{\xi}_J(0) \rightarrow 0$ in the limit $\bar{\xi}_2(0) \rightarrow 0$, so that we can write $\bar{\xi}_J(0) \rightarrow [\bar{\xi}_2(0)]^\alpha$, with $\alpha = \alpha[J]$. So we may consider the general case:

$$\bar{\xi}_J(0) = B_J [\bar{\xi}_2(0)]^{\alpha[J]}. \quad (18)$$

Let us consider the different possibilities for $\alpha = \alpha[J]$ in the above series (16). When $\alpha > J - 1$ the initial conditions are *forgotten*, as the leading-order effect of the evolution is still the hierarchical term, S_J^G , which dominates the evolution. In the more general case, the contribution to $\bar{\xi}_J$ from Non-Gaussian initial correlations of order larger than J are suppressed by powers of the growth factor D and they only become important at late times. When $J/2 < \alpha < J - 1$ we have quasi-Gaussian but non-hierarchical initial conditions. The evolution in $\bar{\xi}_J$ has a dominant non-hierarchical term that grows as D^J , while the hierarchical term grows as $D^{2(J-1)}$ and may not become significant until $\bar{\xi}_2 \sim 1$. Note that, as pointed out by FS94, there is an additional Non-Gaussian term that grows as D^{J+1} and, for the skewness ($J = 3$), it contributes directly to $S_3 \equiv \bar{\xi}_3/\bar{\xi}_2^2$ so that $S_3 \neq S_3^G$ at all times. When $\alpha = J/2$, as in the dimensional scaling where $\bar{\xi}_J(0) \simeq \bar{\xi}_2(0)^{J/2}$, both terms that grow as D^4 depend on $\bar{\xi}_2^2$ and their total amplitude is $S_3^G + 3/2 d_2$. If $\alpha < J/2$ there are strongly NGIC that dominate the evolution as far as $\bar{\xi}_2$ is small (*i.e.*, on large scales).

Here we will concentrate on the $\alpha = J/2$ case, the transition to the strongly NGIC. For the dimensional scaling which typically arises in topological defects models such as textures, we have,

$$\bar{\xi}_J = B_J \bar{\xi}_2^{J/2}, \quad (19)$$

where the B_J amplitudes are constants and have been predicted to be of order unity (see Turok and Spergel 1991, Gaztañaga and Mähönen 1996).

3.1 The Spherical Collapse Model Results

In the SC model, it is straightforward to work out the perturbation expansion. We can proceed as in Eq.[11] by just keeping track of the dominant terms, as we do not need to solve any additional equations. We represent the different orders in the expansion of the cumulants following the notation introduced in Paper I:

$$\sigma^2 = \sum_i s_{2,i} \sigma_i^2 = \sigma_1^2 + s_{2,3} \sigma_3^2 + s_{2,4} \sigma_4^2 + \dots \quad (20)$$

$$\begin{aligned} S_J &= \sum_i S_{J,i} \sigma_i^2 = \dots + S_{J,-1} \sigma_1^{-1} + S_{J,0} \\ &+ S_{J,1} \sigma_1^1 + \dots, \end{aligned} \quad (21)$$

and we find for the first non-vanishing perturbative contributions:

$$\begin{aligned} s_{2,3} &= \left[\frac{S_3^G}{3} - 1 \right] B_3 \\ s_{2,4} &= 3 - \frac{4}{3} S_3^G - \frac{5}{18} (S_3^G)^2 + \frac{S_4^G}{4} \\ &+ \left[1 - \frac{S_3^G}{2} - \frac{(S_3^G)^2}{12} + \frac{S_4^G}{12} \right] B_4 \\ S_{3,-1} &\equiv S_3^{(0)} = B_3 \\ S_{3,0} &= S_3^G - 2 \left[\frac{S_3^G}{3} - 1 \right] B_3^2 + \left[\frac{S_3^G}{2} - 1 \right] B_4 \\ S_{3,1} &= \left[\frac{S_3^G}{6} - \frac{17}{18} (S_3^G)^2 + \frac{5}{8} S_4^G \right] B_3 \\ &+ \left[3 - 2 S_3^G + \frac{(S_3^G)^2}{3} \right] B_3^3 \\ &+ \left[-4 + \frac{8}{3} S_3^G - \frac{(S_3^G)^2}{6} - \frac{S_4^G}{6} \right] B_3 B_4 \\ &+ \left[1 - \frac{2}{3} S_3^G - \frac{(S_3^G)^2}{12} + \frac{S_4^G}{8} \right] B_5 \\ S_{4,-2} &\equiv S_4^{(0)} = B_4 \\ S_{4,-1} &= 4 S_3^G B_3 + [3 - S_3^G] B_3 B_4 + \left[\frac{2}{3} S_3^G - 1 \right] B_5 \\ S_{4,0} &= S_4^G + \left[3 + 7 S_3^G - \frac{14}{3} (S_3^G)^2 + \frac{3}{2} S_4^G \right] B_3^2 \\ &+ \left[-1 - \frac{10}{3} S_3^G + \frac{(S_3^G)^2}{6} + \frac{5}{4} S_4^G \right] B_4 \\ &+ \left[6 - 4 S_3^G + \frac{2}{3} (S_3^G)^2 \right] B_3^2 B_4 \end{aligned}$$

| SC | Unsmoothed | | Smoothed | |
|------------|--------------|---------------|---------------|---------------|
| NGIC | $\gamma = 0$ | $\gamma = -1$ | $\gamma = -2$ | $\gamma = -3$ |
| $B_J = 1$ | $n = -3$ | $n = -2$ | $n = -1$ | $n = 0$ |
| $s_{2,3}$ | 0.62 | 0.29 | -0.05 | -0.38 |
| $s_{2,4}$ | 1.87 | 0.74 | 0.44 | 0.98 |
| $s_{2,5}$ | 3.36 | 0.60 | -0.05 | -1.05 |
| $S_{3,0}$ | 5.05 | 4.21 | 3.38 | 2.55 |
| $S_{3,1}$ | 7.26 | 3.91 | 1.55 | 0.19 |
| $S_{3,2}$ | 23.53 | 7.37 | 1.18 | 0.20 |
| $S_{4,-1}$ | 19.81 | 16.14 | 12.48 | 8.81 |
| $S_{4,0}$ | 85.88 | 52.84 | 28.31 | 12.27 |
| $S_{4,1}$ | 332.51 | 128.51 | 32.83 | 2.70 |

Table 1. Values of the higher-order perturbative contributions in the SC model from NGIC with $B_J = 1$ for the unsmoothed ($n = -3$) and smoothed ($n = -2, -1, 0$) density fields for a top-hat window and a power-law power spectrum.

$$\begin{aligned}
 & + \left[-3 + \frac{3}{2} S_3^G + \frac{(S_3^G)^2}{4} - \frac{S_4^G}{4} \right] B_4^2 \\
 & + \left[-3 + 3 S_3^G - \frac{2}{3} (S_3^G)^2 \right] B_3 B_5 \\
 & + \left[1 - \frac{5}{6} S_3^G - \frac{(S_3^G)^2}{18} + \frac{S_4^G}{6} \right] B_6 \\
 S_{5,-3} & \equiv S_5^{(0)} = B_5 \\
 S_{5,-2} & = 5 S_3^G B_3^2 + \frac{20}{3} S_3^G B_4 - 4 \left[\frac{S_3^G}{3} - 1 \right] B_3 B_5 \\
 & + \left[\frac{5}{6} S_3^G - 1 \right] B_6 \\
 S_{6,-4} & \equiv S_6^{(0)} = B_6 \\
 S_{6,-3} & = 20 S_3^G B_3 B_4 + 10 S_3^G B_5 - 5 \left[\frac{S_3^G}{3} - 1 \right] B_3 B_6 \\
 & + \left[S_3^G - 1 \right] B_7. \tag{22}
 \end{aligned}$$

We have chosen to write the expressions as a function of S_J^G , the tree-level hierarchical coefficients for GIC, so that when $B_J = 0$, one immediately recovers the Gaussian results. This is possible because, as mentioned in previous sections, the Gaussian tree-level contains all the information of the SC model (see *e.g.*, Appendix A1 in Paper I). Note that this includes both the smoothed and the unsmoothed case, by just replacing the correct value of n or γ_p in S_J^G . We stress that, unlike the case of GIC, odd powers in the linear variance also contribute to the cumulants for generic NGIC as already pointed out in recent papers (see FS94, CB96).

Note that in Eq.[22], there are two types of contributions. First, there are terms that arise as a result of the non-linear gravitational evolution alone ($\sim S_J^G$), which are not coupled to the IC, B_J and thus which contribute in the same way as for GIC. Second, there are those terms coupled

to the IC ($\sim B_J$) which depend on the specific Non-Gaussian model for the IC.

It is natural to introduce the non-linear *dimensional* ratios for the texture-like NGIC (see Eq.[2]),

$$B_J^{NL} = \sum_i B_{J,i} \sigma_i^i = B_{J,0} + B_{J,1} \sigma_1^1 + \dots, \tag{23}$$

Notice that the linear term ($\sim \mathcal{O}(\sigma_\dagger^1)$) remains equal to its initial value (contrary to the leading order to the S_J ratios, see Eq.[3]), while the σ -corrections (*i.e.*, the $\mathcal{O}(\sigma_\dagger)$ terms) only appear when non-linear gravitational evolution sets up. In particular, we have to keep $J-2$ corrective terms in order to include the purely gravitational term (not coupled to the IC), $\sim S_J^G$. Note that one has to include this hierarchical term to get an accurate estimate of the B_J^{NL} , as its contribution increases with decreasing scale (see Figs 7 & 8 for $S_J = B_J \sigma^{2-J}$).

$$\begin{aligned}
 B_{3,1} & = S_3^G + \frac{1}{2} (3 - S_3^G) B_3^2 + \left(\frac{S_3^G}{2} - 1 \right) B_4 \\
 B_{4,1} & = 4 S_3^G B_3 + 2 \left(1 - \frac{S_3^G}{3} \right) B_3 B_4 + \left(\frac{2}{3} S_3^G - 1 \right) B_5 \\
 B_{4,2} & = S_4^G + 3 \left[1 + S_3^G - \frac{10}{9} (S_3^G)^2 + \frac{S_4^G}{2} \right] B_3^2 \\
 & + \left[2 - \frac{14}{3} S_3^G - \frac{1}{9} (S_3^G)^2 + \frac{3}{2} S_4^G \right] B_4 \\
 & + \left[3 - 2 S_3^G - \frac{1}{3} (S_3^G)^2 \right] B_3 B_4 \\
 & + \left[-2 + S_3^G + \frac{1}{6} (S_3^G)^2 - \frac{1}{6} S_4^G \right] B_4^2 \\
 & - 2 \left[-1 + S_3^G - \frac{2}{9} (S_3^G)^2 \right] B_3 B_5 \\
 & + \left[1 - \frac{5}{6} S_3^G - \frac{1}{18} (S_3^G)^2 + \frac{1}{6} S_4^G \right] B_6 \tag{24}
 \end{aligned}$$

Notice that for most of the cosmological models, quasi-linear scales (where PT applies) have an *effective* spectral index n_{eff} , associated to a power-law power spectrum, $P(k) \sim k^{n_{eff}}$, within the range $n_{eff} \in [-1, -2]$, for which $S_3^G \approx 3$. This means that, for most of the models, the second term in $B_{3,1}$ & $B_{4,1}$ have a negligible contribution.

Table 1 shows the results for the NGIC for $B_J = 1$ and different power indexes. These are to be compared with the GIC case in Table 2 of Paper I.

Figs 1 and 2 show the departures from the tree-level amplitudes for the variance, skewness and kurtosis up to the 2nd and 3rd perturbative order respectively, as the linear rms fluctuation grows. It is seen how the 2nd order contribution (first corrective term) for the variance exhibits a cancellation of non-linearities for $n \approx -1$ which tends to disappear when the linear rms density fluctuation approaches unity, once the next perturbative order (second corrective term) is included, as shown in Fig 2. We interpret that this is due to the fact that, here, unlike the case for GIC, the initial conditions still dominate the 2nd perturbative contribution in the evolved variance and further (3rd order) contributions change this picture since gravitational evolution takes over the initial conditions. Put it another way, it takes longer for the gravitational evolution to erase the trace of strongly NGIC.

On the other hand, for the skewness and kurtosis we

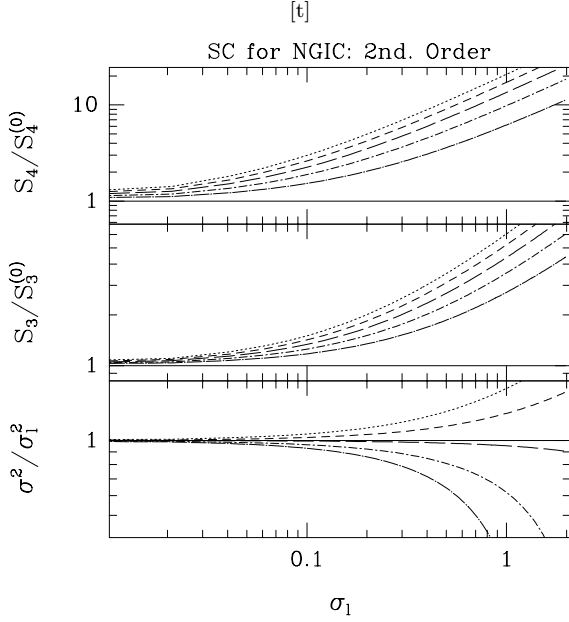


Figure 1. Departures from the tree-level contributions as the linear *rms* fluctuation grows, for the variance, skewness and kurtosis of the density field as predicted by the SC model up to the 2nd non-vanishing perturbative contribution (first corrective term) for different values of the spectral index: the dotted line shows the $n = -3$ (unsmoothed) case, and the short-dashed ($n = -2$), long-dashed ($n = -1$), dot short-dashed ($n = 0$), dot long-dashed ($n = 1$) depict the behavior for the smoothed density field. The solid line shows the tree-level values (or linear term for the variance) as a reference. It is shown the case of Non-Gaussian initial conditions with $B_J \approx 1$.

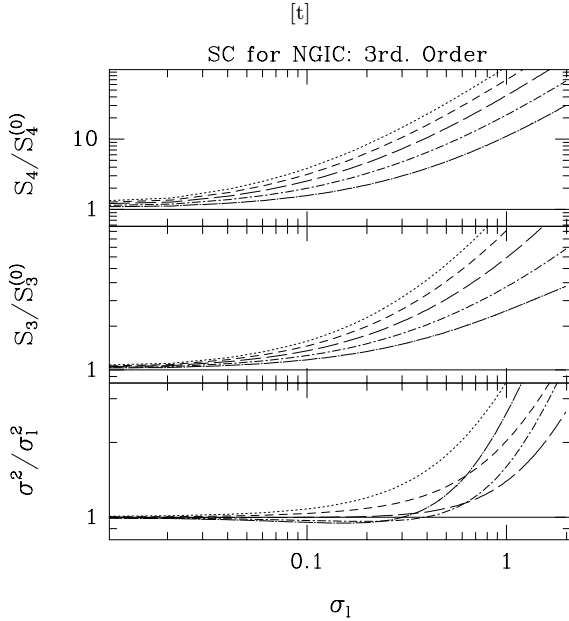


Figure 2. Same as Fig 1, when the 3rd perturbative contribution is taken into account.

see a significant change from the Gaussian case that holds in the 2nd and 3rd order analysis: strong non-linear effects are found for any value of the spectral index, contrary to what happened for GIC where there was a characteristic index $n \simeq 0$, where non-linear effects vanished. This difference must be due to the strong Non-Gaussian character of the initial conditions. In fact, by looking at the expressions for S_3 and S_4 for dimensional NGIC (see *e.g.*, Eq.[22] above) we see that, unlike the case of the variance, the higher-perturbative orders are completely coupled to the initial conditions ($\sim B_J$ terms), so that, even for the smallest scales, deviations from the PT predictions for Gaussian initial conditions (where gravitational evolution clearly dominates) must show up. This deviation from the Gaussian prediction on small scales is realized as a shift from the Gaussian values in the hierarchical contributions (order zero in σ , $S_{J,0}$).

3.2 Comparison with the Gaussian Case

We have explored the non-linear corrections to the 1-point cumulants of the density field, within the SC model, for Gaussian (in Paper I) and Non-Gaussian dimensional initial conditions separately. The aim of this section is to provide a direct way of comparing the predictions in both cases so as to get a further insight on how the choice of initial conditions changes the non-linear evolution.

To simplify the comparison, we shall assume that the B_J coefficients (see *e.g.*, Eq.[2]), are all equal, which is roughly what is expected from analytic models for Topological defects. We denote $\beta \equiv B_J$ as the *Non-Gaussian strength*. While the results in Table 1 assume $\beta = 1$, we will now display the non-linear corrections as a function of β . We shall concentrate on the coefficients of even corrections in powers of σ ($s_{2,4}$, $S_{J,0}$), as the odd corrections vanish for GIC. Note nevertheless that these latter could be dominant contributions when studying the overall non-linear effect for NGIC. Using Eq.[22], we find for top-hat smoothing and a power-law spectrum:

$$\begin{aligned}
 s_{2,4} &= \frac{1909}{1323} + \frac{143}{126} \gamma + \frac{11}{36} \gamma^2 + \left(\frac{1705}{3969} + \frac{26}{63} \gamma + \frac{\gamma^2}{9} \right) \beta \\
 S_{3,0} &\equiv S_3^{(0)} = \frac{34}{7} + \gamma + \left(\frac{10}{7} + \frac{\gamma}{2} \right) \beta - \left(\frac{26}{21} + \frac{2}{3} \gamma \right) \beta^2 \\
 S_{4,0} &\equiv S_4^{(0)} = \frac{60712}{1323} + \frac{62}{3} \gamma + \frac{7}{3} \gamma^2 \\
 &+ \left(\frac{188105}{3969} + \frac{550}{21} \gamma + \frac{41}{12} \gamma^2 \right) \beta \\
 &- \left(\frac{12841}{1323} + \frac{253}{21} \gamma + \frac{13}{6} \gamma^2 \right) \beta^2 \\
 &+ \left(\frac{338}{147} + \frac{52}{21} \gamma + \frac{2}{3} \gamma^2 \right) \beta^3. \tag{25}
 \end{aligned}$$

The case of GIC is reproduced by just setting $\beta = 0$, while one could expect $\beta \simeq 1$ for a defect model. Recall that $\gamma = -(n+3)$.

Figures 3-5 show the deviations from the Gaussian perturbative contributions in the Non-Gaussian model as a function of the *Non-Gaussian strength* β , for several smoothing values, n . They show the robustness of the arguments drawn from the $\beta = 1$ case (see Table 1). The Non-Gaussian contributions are larger than the Gaussian one for $1 \gtrsim \beta \gtrsim$

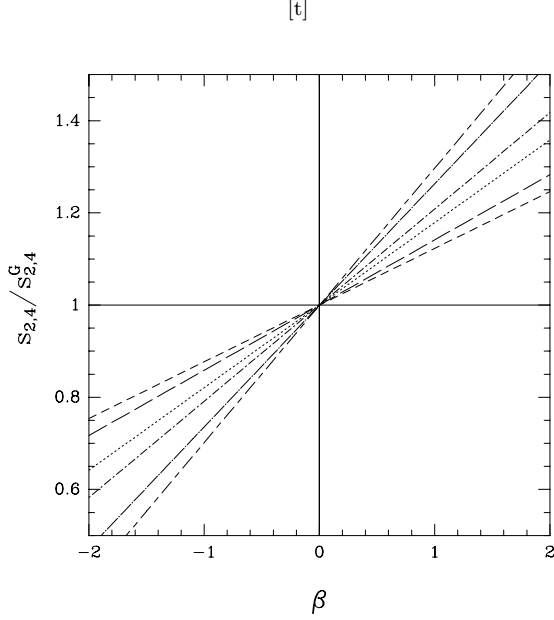


Figure 3. Departures from the Gaussian behavior in the coefficient $s_{2,4}$ of the σ^4 correction to the linear variance as a function of the Non-Gaussian strength $\beta = B_J$. The values displayed correspond to $n = -0.5$ (dotted line), $n = -1$ (short-dashed), $n = -1.5$ (long-dashed), $n = -2$ (dot short-dashed), $n = -2.5$ (dot long-dashed), $n = -3$ (short-dashed long-dashed).

0. For positive NGIC ($\beta > 0$), this trend is typically enhanced when smoothing effects increase.

However, for negative values of the Non-Gaussian strength β , the behavior changes. It is found that the variance falls below the Gaussian value, while the Non-Gaussian S_J coefficients may overestimate or underestimate the Gaussian prediction depending on the scales (effective spectral index) we are looking at. Typically it underestimates the Gaussian value on quasi-linear scales.

The general behavior found for the variance ($s_{2,4}$) seems to be in qualitative agreement with the conclusions drawn by FS94 which pointed out that a larger (lower) variance than the Gaussian one is expected for models with positive (negative) initial skewness (see also Moscardini *et al.* 1993). But note that this trend changes when $S_3^G < 3$, since, then $s_{2,3} < 0$, which is the leading term in the variance (see Eq.[22]). This was not detected by FS94 because they did not include smoothing effects. Thus, for $n > -8/7 \approx -1.14$ or $\gamma < -1.85$, there is a change in this trend, with lower variance for more positive skewness. In observations and also in CDM models (see Gaztañaga & Baugh 1998), the spectral index is $n \lesssim -1$ in the weakly non-linear scales, going to $n > -1$ on large scales. This will produce a characteristic change in the shape (see Figure 6 below).

For $S_{3,0}$, a critical index is observed at $n = -8/7 \approx -1.14$ ($\gamma = -13/7$) below which the Non-Gaussian hierarchical amplitude has a maximum as a function of β which depends on the value of n (see inset in Fig 4). For $n > -8/7 \approx -1.14$ there is instead a minimum as a function of β . These bounds could be of interest when interpreting the estimations of S_3 from observations. Given a value of

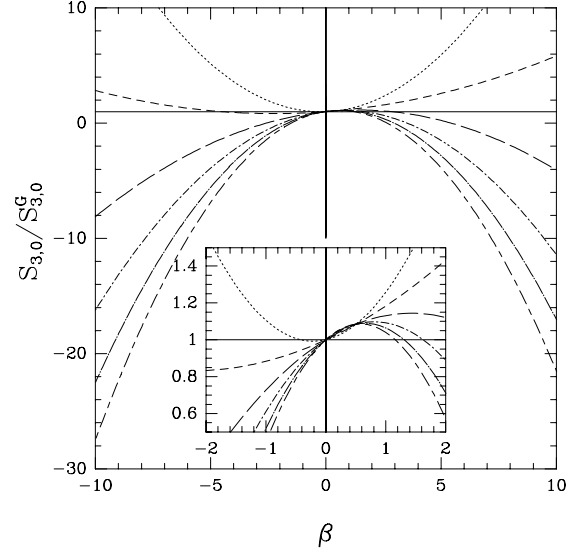


Figure 4. Same as Fig. 3 for the hierarchical contribution to the skewness, $S_{3,0}$. The inset in the bottom shows a detail of the plot for a shorter range of the Non-Gaussian parameter β .

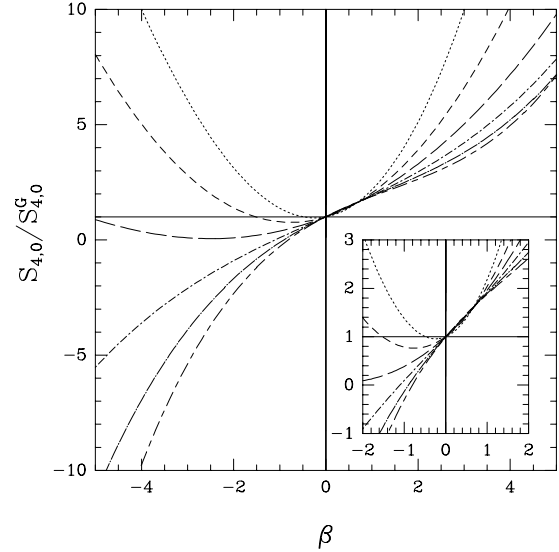


Figure 5. Same as Fig. 3 for the hierarchical contribution to the kurtosis, $S_{4,0}$.

the index γ , there is a maximum ($\gamma > -13/7$) or minimum ($\gamma < -13/7$) in the non-linear coefficient at:

$$\beta_m = \frac{3(20 + 7\gamma)}{8(13 + 7\gamma)} \quad (26)$$

for which the ratio is:

$$\left. \frac{S_{3,0}}{S_{3,0}^G} \right|_{\beta_m} = \frac{7(2192 + 1624\gamma + 245\gamma^2)}{32(442 + 329\gamma + 49\gamma^2)} \quad (27)$$

For $S_{4,0}$ we can also see some bounds (which depend on the spectral index) that could be of practical interest.

3.3 Comparison with N-body Results

The above predictions are in good agreement with the N-body simulations depicted in Figs 6-8. The N-body results (symbols with error-bars from 3 realizations) are from Gaztañaga and Mähönen (1996). A non-linear sigma model was used for the texture dynamics, which was stopped at $\sigma_8 = 0.1$. Density perturbations were mapped by 100^3 particles to produce the initial conditions for a gravitational N-body simulation. The density fluctuations were then evolved by a P³M-code (Efstathiou & Eastwood 1981, Efstathiou *et al.* 1988) until they reach $\sigma_8 = 1.0$.

We first fit a model for initial conditions $\xi_J(0)$ using the statistics of the initial density fluctuations in the simulations obtained from a map (which assumes $\Omega = 1$) of the texture dynamics (non-linear sigma model) at $\sigma_8 = 0.1$ (*e.g.*, 10 expansion factors before now: $\sigma_8 = 1.0$). For the initial variance we use a numerical fit, which will be scaled with $a = D$ to be the linear variance. We corrected this initial values from the grid shot-noise, and the results are the average of 3 realizations, which explains why the SC predictions are not smoothed in the Figures. For the higher-order cumulants of the IC, a good match for $R \gtrsim 10 h^{-1}$ Mpc is given by the dimensional scaling $\bar{\xi}_J = B_J \sigma^J$, with $B_J \simeq 0.5$. This model for the initial conditions is shown as the upper dotted lines in the plots for the S_J amplitudes (only larger scales are shown for clarity, smaller scales are dominated by large shot-noise fluctuations).

For $n \simeq -1$ ($\gamma \simeq -2$), the prediction for $B_J = 0.5$ is,

$$\begin{aligned} \sigma^2 &\approx \sigma_l^2 - 0.02 \sigma_l^3 \\ B_3^{NL} &\approx 0.5 + 3.1 \sigma_l \\ B_4^{NL} &\approx 0.5 + 6.2 \sigma_l + 19.7 \sigma_l^2 \end{aligned} \quad (28)$$

We remark that a PT prediction for B_J^{NL} must keep at least $J - 2$ corrective terms to the linear prediction to include the (hierarchical) purely gravitational term, S_J^G (see Eq.[24]). This means that to yield a meaningful prediction for the skewness and kurtosis we have to include one and two (non-linear) corrective terms, respectively, to the linear theory prediction. In practice, n (or, equivalently, γ) is a function of the scale R , so that the coefficients of the non-linear corrections above (*e.g.*, $s_{2,3}$) are a function of the local slope, γ . This slope is obtained numerically from the initial variance.

For the variance, $\xi_2 \equiv \sigma^2$, we find in Figure 6 a good agreement between the the simulation output (for $\sigma_8 = 1.0$, open squares) and the SC prediction for the leading contribution to the non-linear variance: $s_{2,3}$ (short-dashed line). The agreement extends up to the scales where the shot-noise dominates the correlations (beyond the point where $\sigma \approx 0.5$). In particular, the negative contribution predicted for the variance in $s_{2,3}$ is clearly in agreement with the behavior measured in the simulations. The latter is related to the fact that, contrary to the Gaussian case (see Paper I, §5.2), the variance has a critical effective index, $n = -8/7$ for which the non-linear contributions change sign (see Fig 1). This has nothing to do with the previrialization effect found for GIC (since the SC model is unable to account for this effect, see Paper I, §5.2) but rather with the fact that the variance is still dominated by the IC which push the variance towards lower values. The prediction for the next contribution to the variance $s_{2,4}$ for the NGIC (long-dashed line) and the Gaussian IC (dotted line), shows that

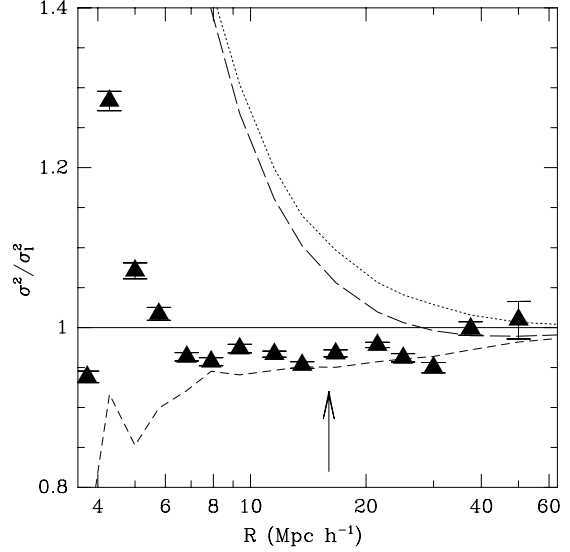


Figure 6. The ratio of the non-linear to the linear variance σ^2/σ_l^2 in texture-like non-Gaussian models. Displayed are the predictions from the SC model including $s_{2,3}$ (short-dashed line) and $s_{2,4}$ (long-dashed), which is dominated by the Gaussian contribution (shown as the dotted line). The N-body simulation for $\sigma_8 = 1.0$ (filled triangles) shows a non-linear variance below the linear one on all quasi-linear scales in remarkable agreement with the SC prediction for the first non-linear contribution $s_{2,3}$.

this term is dominated by the Gaussian contribution (that independent of B_J), with a behavior similar to the one found for GIC (see Paper I, §5.2), *i.e.*, positive contributions to the variance on all scales. A clear departure of the variance including the first non-linear correction ($s_{2,3}$), with respect to the prediction once the second correction is included ($s_{2,4}$) suggests the point beyond which the perturbative approach should break down (see arrow in Fig 6). The second non-linear ($s_{2,4}$) correction to the variance, seems to be dominated by the tidal contributions missed in the SC model prediction, as displayed in Fig 6. Note nevertheless the similarity of this effect to the one found in Figure 6 of Paper I. There, the first order (non-linear) correction to the variance in the APM simulations also gives a much better agreement than the second order correction. This might indicate that 2-loop calculations have stronger tidal contributions, so that the SC model is a poorer approximation for higher-order loops.

On the other hand, in the plots concerning the hierarchical amplitudes S_J , the lower dotted lines are the linear theory predictions, which only approach the non-linear results at the larger scales, $R \simeq 40 h^{-1}$ Mpc ($\sigma \lesssim 0.1$), where they do better than the GIC predictions, but are not as good as the NGIC predictions.

There is an excellent agreement between the SC model predictions for S_J with those from the N-body simulations up to the point where the prediction including the $S_{J,1}$ contribution significantly deviates from that up to the hierarchical term, $S_{J,0}$ (which includes the purely gravitational term, S_J^G). This means that for the skewness, S_3 (kurtosis, S_4), the SC result is reliable as long as the prediction including the

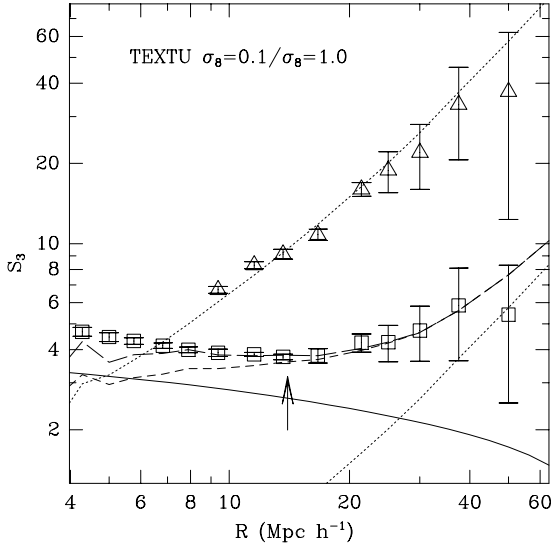


Figure 7. The hierarchical skewness, S_3 , for texture-like non-Gaussian models. The triangles show the initial conditions ($\sigma_8 = 0.1$), which are fitted well by the dimensional scaling $S_3 = B_3/\sigma$, shown as the upper dotted line. Squares show S_3 for a later output: $\sigma_8 = 1.0$. The SC predictions for the $\sigma_8 = 1$ output are shown as short-dashed (including the second order contribution) and long-dashed line (including the third order). The continuous line shows the corresponding tree-level PT prediction for Gaussian initial conditions. The lower dotted lines correspond to the linear theory prediction.

2nd (3rd) and the 3rd (4th) perturbative contributions are in rough agreement. This point is reached approximately for $\sigma \simeq 0.5$, which is shown as an arrow in Figs. 7 & 8. Notice that for NGIC, loop corrections enter at the same order (in σ) as tree-level corrections. Note also the deviation from the Gaussian prediction on quasi-linear scales which shows up as a shift from the Gaussian values, as mentioned above and predicted in Eq[22] (order zero in σ , $S_{J,0}$).

Similar results are found for higher-order moments, which have also been used to check the initial correlations, $B_J \simeq 0.5$ up to $J = 6$.

3.4 Comparison with Exact PT

The analytic PT calculations available in the literature for Non-Gaussian initial conditions refer only to the variance, σ , the skewness S_3 (see FS94) and the dimensional kurtosis, B_4 (see CB96) for the *unsmoothed* fields. We will now compare our results to those of the exact (*non-local*) calculation.

3.4.1 The Variance in exact PT

For the unsmoothed variance FS94 find:

$$\sigma^2 = \sigma_i^2 + \frac{13}{21} \xi_3^l + \frac{4}{7} I[\xi_3^l] + \mathcal{O}(\sigma_i^4) \quad (29)$$

where ξ_3^l is the linear 3-point function: $\xi_3^l \equiv \langle \delta_i^3 \rangle_c = D^3 \xi_3(0)$ and $I[\xi_3^l]$ stands for some multipole integral of the linear three-point function contributing to the one-loop order. In particular, we define,

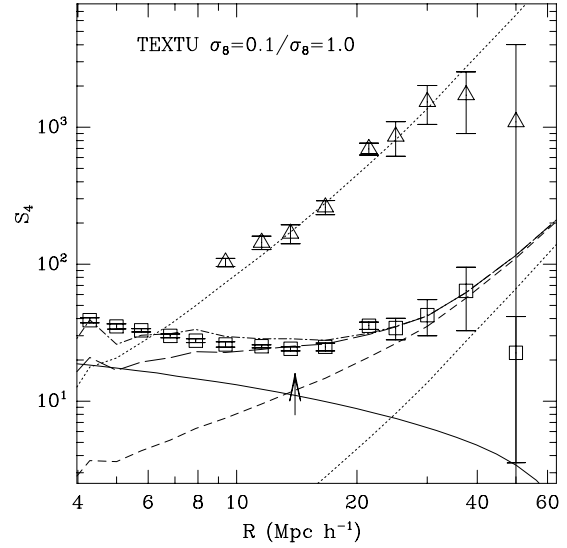


Figure 8. The hierarchical kurtosis, S_4 , for texture-like non-Gaussian models. Symbols and lines as in Figure 7. The new line in the plot (dot long-dashed) displays the SC prediction including the 4th perturbative contribution. In this case the initial conditions are fitted to the corresponding dimensional relation $S_4 = B_4/\sigma^2$.

$$I[f(\mathbf{x}, \mathbf{x}')] = \int \frac{d^3 \mathbf{x}}{4\pi} \frac{d^3 \mathbf{x}'}{4\pi} \frac{(3 \cos^2 \theta - 1)}{\mathbf{x}^3 \mathbf{x}'^3} f(\mathbf{x}, \mathbf{x}'), \quad (30)$$

with $\cos \theta = \mathbf{x} \cdot \mathbf{x}' / |\mathbf{x}| |\mathbf{x}'|$. That integral term, $I[\xi_3^l]$, competes, at the same order, with the tree-level amplitude in the perturbative expansion for dimensional IC. As a result, though the tree-level amplitudes remain (local) shearless, the tidal one-loop contribution cannot be exactly recovered by the SC model. In particular, from the SC model we found for the evolved variance,

$$\sigma^2 = \sigma_i^2 + \left(\frac{S_3^G}{3} - 1 \right) B_3 \sigma_i^3 + \mathcal{O}(\sigma_i^4), \quad (31)$$

where here $B_J = \xi_J^l / \sigma_i^J$ denote the dimensional amplitudes, and $S_3^G = 34/7$ (the tree-level skewness for GIC). Replacing the latter number in the expressions above, we see that our results within the SC model are able to recover all the terms given by the exact calculation up to the one-loop tidal-induced term dependent on the initial three-point function, *e.g.*, $\frac{4}{7} I[\xi_3^l]$. Note that SF94 typically find (see their Table 1) that the coefficients $\eta_J \equiv I[\xi_J^l] / \xi_J$ resulting from the multipole integration are smaller than unity, $\eta_J \lesssim 0.2$, thus typically smaller than the monopole contribution. As mentioned above this is not totally surprising as correlations typically decrease with distance, thus reducing the contribution in non-spherical geometries. Furthermore, note that the SC results above provides with the smoothed generalization of the FS94 results (up to tidal effects), *e.g.*,

$$\langle \delta^2 \rangle = \sigma_i^2 + \left(\frac{13}{21} + \frac{\gamma}{3} \right) \xi_3^l + \dots \quad (32)$$

The general behavior found for the variance seems to be in qualitative agreement with the conclusions drawn by FS94 which pointed out that a larger (lower) variance than the

Gaussian one is expected for models with positive (negative) initial skewness (see also Moscardini *et al.* 1993). But note that this trend changes when $S_3^G < 3$, i.e., when $s_{2,3} < 0$, which is the leading term in the variance (see Eq.[22]). This was not detected by FS94 because they did not include smoothing effects. Thus, for $n > -8/7 \approx -1.14$ or $\gamma < -1.85$, there is a change in this trend, with lower variance for more positive skewness. In observations and also in CDM models (see Gaztañaga & Baugh 1998), the spectral index is $n \lesssim -1$ in the weakly non-linear scales, going to $n > -1$ on large scales. This will produce a characteristic change in the shape (see Figure 6).

Within SC model the reason for this qualitative change (lower or higher variance for more positive skewness) lies in the combination of smoothing effects and the transformation from Lagrangian to Eulerian coordinates, which reduce non-linearities. Indeed, the negative term in $s_{2,3} = (S_3^G/3 - 1) B_3$, which makes the cancellation possible, comes from the Lagrangian to Eulerian transformation. While smoothing effects, can reduce the value of S_3^G and change the relative sign.

Note the repeated appearance of a critical index $n \simeq -8/7 \approx -1.14$ ($\gamma \simeq -1.85$) in the SC model predictions for the cumulants (see also Paper I). At this index, the corrections to the variance are minimal for GIC and change sign for NGIC. Furthermore, the skewness coefficient $S_{3,0}$ also shows a critical behavior (see §3.2) for that particular value. This critical index happens to correspond to the solution to the equation $S_3^G = 3$, which lies close to the observational values of both S_3 (see Gaztañaga 1994) and n itself (Gaztañaga & Baugh 1998) in the quasi-linear regime.

3.4.2 Skewness & Kurtosis in exact PT

Similarly, for the skewness, FS94 give,

$$S_3 = \frac{\xi_3^l}{\sigma_l^4} + \frac{34}{7} + \frac{10}{7} \frac{\xi_4^l}{\sigma_l^4} - \frac{26}{21} \frac{(\xi_3^l)^2}{\sigma_l^6} + \frac{6}{7} \frac{I[\xi_4^l]}{\sigma_l^4} - \frac{8}{7} \frac{\xi_3^l I[\xi_3^l]}{\sigma_l^6} + \mathcal{O}(\sigma_l) \quad (33)$$

with the tidal terms expressed as integrals $\sim I[\xi_3^l], I[\xi_4^l]$ of the linear three- and four-point functions respectively. Recalling the corresponding expression for the skewness in the SC model,

$$S_3 = \frac{B_3}{\sigma_l} + S_3^G - 2 \left(\frac{S_3^G}{3} - 1 \right) B_3^2 + \left(\frac{S_3^G}{2} - 1 \right) B_4 + \dots \quad (34)$$

we see again how the SC approximation exactly recovers all the local terms, but not the tidal or non-local integrals. Note that, in this case, the two tidal contributions to the reduced cumulants appear at the one-loop order as differences in the J -point functions, leading in most of the cases (see FS94, Table 1) to a marginal contribution to the SC prediction.

Finally, we turn to the result derived by CB96, for the dimensional (non-linear) kurtosis, B_4^{NL} for an arbitrary Non-Gaussian density field. They find,

$$B_4^{NL} = B_4 + B_{4,1} \sigma_l + \mathcal{O}(\sigma_l^2) \quad (35)$$

being,

$$B_{4,1} = \frac{47}{21} B_5 + \frac{136}{7} B_3 - \frac{26}{21} B_3 B_4$$

$$+ \frac{8}{7} \left(B_5 \frac{I[\xi_5^l]}{\sigma_l^5} - B_4 B_3 \frac{I[\xi_3^l]}{\sigma_l^3} \right) \quad (36)$$

From the SC approximation we find a similar expression (see Eq.[24]), which after replacing $S_3^G = 34/7$, matches the PT result for the tree-level contribution while failing to reproduce the one-loop tidal terms. These involve some integrals of the initial J -point functions, just as the case of the skewness commented above. Again, we expect this tidal contribution to generically yield a marginal net correction to the SC model prediction ($\eta_J \lesssim 0.2$).

Note again that all the exact results mentioned above correspond only to the *unsmoothed* cumulants. In the present context, the local contribution can be easily extended for the smoothed case. The *smoothed* predictions are implicitly given in equations (22) and Table 1 and tend to yield smaller non-linearities, similar to what was found in Paper I for GIC.

3.5 Predictions for the isocurvature CDM cosmogony

As an interesting working example, consider the isocurvature CDM cosmogony presented recently by Peebles (1998). In the particular model presented Peebles used for the initial conditions the following parameters: $B_3 = D_3 \simeq 2.5$, $B_4 = D_4 \simeq 9.9$ and $\gamma = -2\epsilon = -1.2$. From Eqs.[22],[24] we have that the leading order non-linear corrections to σ^2 , $B_3^{NL} = S_3 \sigma$ and $B_4^{NL} = S_4 \sigma^2$, in terms of the linear *rms* fluctuation, σ_l , are:

$$\begin{aligned} \sigma^2 &\approx \sigma_l^2 + 0.55 \sigma_l^3 \\ B_3^{NL} &\approx 2.5 + 9.8 \sigma_l \\ B_4^{NL} &\approx 9.9 + 98 \sigma_l + 560 \sigma_l^2 \end{aligned} \quad (37)$$

where to estimate the non-linear correction for B_4^{NL} we have assumed $B_5 \simeq 1.6(B_4)^{3/2} \simeq 50$, and $B_6 \simeq 3.3(B_4)^2 \simeq 300$, following the χ^2 distribution. These non-linear corrections are not very sensitive to the values assumed for B_5 and B_6 , as setting them to zero (a very conservative assumption) yields $B_4^{NL} \approx 9.9 + 26 \sigma_l + 250 \sigma_l^2$, which is anyway a very large correction to the linear theory prediction, $B_{4,0} = 9.9$, when $\sigma_l \simeq 1$. We stress that a PT prediction for B_J^{NL} must keep at least $J - 2$ corrective terms to the linear prediction to include the non-negligible purely gravitational term, S_J^G (see Eq.[24]). This can also be seen in Figs 7 & 8 where the SC prediction follows the N-body predictions up to $\sigma_l \lesssim 1$ only when the first and second corrective terms are included in the perturbative expansion of the skewness and kurtosis, respectively.

Note that the Isocurvature CDM model has a much larger non-linear correction for the variance than that of the texture model discussed in §3.3 (see Eq.[28] and also Fig 6), because there, the spectral index, is lower ($n \approx -1$) than in the Isocurvature CDM cosmogony ($n = 2\epsilon - 3 \approx -1.8$, see Peebles 1998). According to the above results, the non-linear corrections to B_J^{NL} are very large (and positive) and linear theory is no longer a good approximation for $\sigma_l \simeq 1$. This is very similar to the situation presented in Figures 7-8 for the texture model, where linear theory only works for $R > 50 h^{-1}$ Mpc, or $\sigma_l < 0.1$. What is more, the non-linear corrections to the B_J^{NL} are typically an order of magnitude larger than the linear values (see Eqs.[28],[37]).

These non-linear corrections should be taken into account when comparing the model with observations in the galaxy catalogues, as in Table 1 of Peebles (1998), where even at the larger scales $\theta \simeq 1$ deg ($R \simeq 10 h^{-1}$ Mpc), one has $\sigma_l \simeq 1$. Thus, for the parameters shown in Eq.[37], the model seems to be incompatible with current observational constraints from galaxy catalogues.

4 DISCUSSION AND CONCLUSIONS

For Gaussian initial conditions (GIC), we found in Paper I, that the Spherical Collapse (SC) model gives the exact tree-level contribution to PT. It was shown that this contribution can be derived by means of a local-transformation of the IC, what is much simpler than the vertex generating function formalism developed by Bernardeau (1994a, 1994b). It was also seen in Paper I that the SC model (in Lagrangian space) also gives an excellent agreement for the hierarchical amplitudes S_J in the loop corrections, as compared with the results derived by Scoccimarro & Frieman (1996a, 1996b) for the exact PT in the diagrammatic approach.

We stress the importance of applying the SC approximation in Lagrangian space. There, the SC model is described by a transformation that *only* depends on the value of the linear field at the same point (what we call a *local-density transformation*). However, when going back to Euler space the density fluctuation (defined at a point) is normalized with a factor which is a function of the (non-linear) variance. Since the variance is a volume average of the two-point correlation function, this factor yields some *non-local* contribution to the cumulants (in Euler space). This *non-local* contribution is missed when introducing the SC model in Euler space *directly*, thus is not surprising that the predictions for the cumulants in the SC approximation in Euler space are a poor estimation of those in exact PT, as the latter are dominated by the non-local (tidal) effects (see Table A2 in Paper I).

For the predictions within the SC model (in Lagrangian space) for the hierarchical ratios, S_J , tidal effects partially cancel out as they seem to contribute roughly hierarchically to the cumulants (see Appendix A2 in Paper I). This is also true for the SC model in Euler space, but the dominance of non-local effects in the cumulants there, yield significantly different S_J ratios to those in exact PT (see Appendix A2 in Paper I). Smoothing effects do not alter substantially this interpretation (at least for a top-hat window).

As the SC model can be easily extended to the smoothed fields, we were able compare the predictions for the higher-order moments from the SC model to those measured in CDM and APM-like N-body simulations, and they turned out to be in very good agreement in all cases up to the scales where $\sigma_l \approx 1$, supporting our view that the tidal effects only have a marginal contribution to the reduced cumulants. Furthermore, the break down of the shearless approximation roughly coincides with the regime for which the perturbative approach itself breaks down, $\sigma \simeq 0.5$. That is, where the contribution of the second and the third perturbative order in the SC model are significantly different.

For non-Gaussian initial conditions (NGIC) the SC recovers all tree-graphs exactly, including all contributions given by the exact PT for the variance, σ , skewness, S_3 ,

and kurtosis, S_4 , up to some non-local integrals, $I[\xi_J]$, involving J -point initial functions. These last integrals arise as a result of the coupling between the asymmetric initial conditions with the tidal forces. We argue that for the hierarchical ratios, S_J , these non-local terms are sub-dominant and tend to compensate each other (*e.g.*, $I[\xi_J] < \xi_J$).

The measured higher-order moments in the N-body simulations with NGIC (with dimensional, texture-like, scaling) turned out to be in good agreement with predictions from the SC model up to the scales for which the perturbative series breaks down (*e.g.*, see Figures 6-8). As mentioned in Paper I there is a critical index, $n_* \in [-1, -2]$, for which tidal effects vanish and the SC is a good approximation even for the variance. This might explain why we find such a good agreement for the variance as compared to the simulations (which have $n \simeq -1$ on weakly non-linear scales). This good agreement is found when using only the leading-order correction $\mathcal{O}[\sigma_l^3]$, and breaks down after including the next term, $\mathcal{O}[\sigma_l^4]$ (see Figure 6). This effect is similar to what we found for GIC when comparing the variance between SC predictions and simulations (Figure 6 of Paper I). This could indicate that 2-loop calculations have stronger tidal contributions, so that the SC is a poorer approximation for higher-order loops.

The general behavior found for the variance seems to be in qualitative agreement with the conclusions drawn by FS94 which pointed out that a larger (lower) variance than the Gaussian one is expected for models with positive (negative) initial skewness (see also Moscardini *et al.* 1993). But note that this trend changes when $S_3^G < 3$ i.e., when $s_{2,3} < 0$, which is the leading term in the variance (see Eq.[22]). This was not detected by FS94 because they did not include smoothing effects. Thus, for $n > -8/7 \approx -1.14$ or $\gamma < -1.85$, there is a change in this trend, with lower variance for more positive skewness (see §3.4).

The SC model predictions for S_J show how the NGIC evolve slowly towards the (Gaussian) gravitational predictions but, even at $\sigma_8 = 1$, are still significantly larger. They show a characteristic minimum with a sharp increase in S_J with increasing scales, just as found by Gaztañaga & Mähönen (1996) in N-body simulations of NGIC. The latter agreement strongly constrains the tidal contributions to the higher-order moments and gives further support to the domain of applicability of the SC model in PT. Thus, the resulting SC predictions for the NGIC show a non-trivial time evolution that can be used to strongly discriminate models of structure formation (see §3.5).

ACKNOWLEDGMENTS

We want to thank Roman Scoccimarro, Francis Bernardeau and Josh Frieman for carefully reading the manuscript and pointing out useful remarks. EG acknowledges support from CIRIT (Generalitat de Catalunya) grant 1996BEAI300192. PF acknowledges a PhD grant supported by CSIC, DGICYT (Spain), projects PB93-0035 and PB96-0925. This work has been supported by CSIC, DGICYT (Spain), projects PB93-0035, PB96-0925, and CIRIT, grant GR94-8001.

5 REFERENCES

- Bernardeau, F., 1992, *ApJ*, 392, 1
Bernardeau, F., 1994a, *A&A* 291, 697
Bernardeau, F., 1994b, *ApJ*, 433, 1
Chodorowski, M.J., Bouchet, F.R., 1996, *MNRAS*, , 279, 557 (CB96)
Efstathiou, G., Eastwood, J.W., 1981, *MNRAS*, 194, 503
Efstathiou, G., Frenk, C.S., White, S.D.M., Davis, M. 1988, *MNRAS*, 235, 715
Fosalba, P., Gaztañaga, E., 1998, *MNRAS*, in Press (Paper I, this issue).
Fry, J.N., 1984, *ApJ*, 279, 499
Fry, J.N., Gaztañaga, E., 1993, *ApJ*, 413, 447
Fry, J.N., Scherrer, 1994, R.J., *ApJ*, 429, 1 (FS94)
Gaztañaga, E. & Baugh, C.M., 1998, *MNRAS*, 294, 229
Gaztañaga, E. & Mähönen, P., 1996, *ApJ.Lett.*, 462, L1
Goroff, M.H., Grinstein, B., Rey, S.J., Wise, M.B., 1986, *ApJ*, 311, 6
Jain, B., Bertschinger, E., 1994, *ApJ*, 431, 495
Juszkiewicz, R., Bouchet, F.R., Colombi, S., 1993 *ApJ.Lett.*, 412, L9
Moscardini, L., Coles, P., Matarrese, S., Lucchin, F., Messina, A., 1993, *MNRAS*, 264, 749
Peebles, P.J.E., 1980, *The Large Scale Structure of the Universe*: Princeton University Press, Princeton
Peebles, P.J.E., 1998, *ApJ*, submitted, astro-ph/9805212
Silk J., Juszkiewicz, R. 1991, *Nature*, 353, 386
Soccimarro, R., Frieman J., 1996a, *ApJS*, 105, 37
Soccimarro, R., Frieman J., 1996b, *ApJ*, 473, 620
Turok, N., Spergel, D.N., 1991, *Phys.Rev.Lett.*, 66, 3093
Weinberg, D.H., Cole, S., 1992, *MNRAS*, 259, 652